Available online at www.sciencedirect.com
ScienceDirect
Journal of Power Sources 161 (2006) 1254–1259
JOURNAL OF POWER SOURCES
www.elsevier.com/locate/jpowsour

Effect of fluoroethylene carbonate additive on interfacial properties of silicon thin-film electrode

Nam-Soon Choi *, Kyoung Han Yew, Kyu Youl Lee, Minseok Sung, Ho Kim, Sung-Soo Kim

Corporate R&D Center, Samsung SDI Co. Ltd., 428-5, Gonse-dong, Giheung-gu, Yongin-si, Gyeonggi-do 446-577, Republic of Korea

Received 3 February 2006; accepted 10 May 2006
Available online 5 September 2006

Abstract

A silicon thin-film electrode (thickness = 200 nm) is prepared by E-beam evaporation and deposition on copper foil. The electrochemical performance of a lithium/silicon thin-film cell is investigated in ethylene carbonate/diethyl carbonate/1.3 M $LiPF_6$ with and without 3 wt.% fluoroethylene carbonate (FEC). The addition of FEC remarkably improves discharge capacity retention and coulombic efficiency. The surface morphology and chemical composition of the solid electrolyte interphase (SEI) formed on the surface of the silicon thin-film electrode after cycling are studied through scanning electron microscopy and X-ray photoelectron spectroscopy analysis. A smoother and more stable SEI layer structure is generated by the introduction of the FEC additive to the electrolyte.
© 2006 Elsevier B.V. All rights reserved.

Keywords: Silicon thin-film electrode; Fluoroethylene carbonate; Surface native layer; Solid electrolyte interface; Lithium-ion battery; Surface morphology

1. Introduction

In order to achieve lithium-ion batteries with high specific energy, some metals that can alloy lithium, such as Al, Si, Sn and Sb, have been investigated as promising negative-electrode (anode) materials. In particular, silicon-based alloys with high theoretical capacity (nearly 4200 mAh g^{-1} for $Li_{22}Si_5$) have been extensively studied as a replacement for graphite, which has the theoretical capacity of 372 mAh g^{-1} [1,2]. Silicon–lithium alloy do not, however, retain its high capacity on prolonged cycling. The major reasons for the poor cycling properties are as follows:

- Cracking/crumbling of active material and the loss of electrical conduction paths by a large volume change of the active silicon phase during the insertion and extraction of lithium; the volume expansion is about 300%, as calculated by 100 × (final volume − initial volume)/(initial volume) [3–5].
- Capacity loss by reductive reaction with the components of the native layer (silicon oxide (–Si–O–Si–) and silanol (–Si–OH)).
- Formation of a solid electrolyte interphase (SEI) layer by reductive decomposition of the electrolyte solution during charge process [6–8].
- A continuous SEI-filming process due to continuous crack formation after the first charge–discharge cycle, which exposes new surfaces to the electrolyte [5].

The characteristics of the SEI layer formed at the silicon| electrolyte interface can be one of the dominant parameters that can influence the kinetics of lithiation–delithiation and the interfacial stability during repeated cycling.

The morphology and composition of the SEI layer depend strongly on the electrolyte components [9–13]. There has, however, been little study of the interfacial phenomena between silicon-based anodes and electrolyte solutions, which is one of the most important factors to be addressed in seeking performance improvement.

To develop a favourable SEI layer at the interface of the silicon thin-film electrode and the electrolyte, electrolyte additives which can decouple the interface and bulk properties of the electrolyte can be introduced in small amounts.

In this work, the change in morphology of the silicon thin-film electrode is observed during lithium alloying/de-alloying. The effects of a fluoroethylene carbonate (FEC) additive on the

* Corresponding author. Tel.: +82 31 210 7575; fax: +82 31 210 7555.
E-mail address: ns75.choi@samsung.com (N.-S. Choi).

0378-7753/$ – see front matter © 2006 Elsevier B.V. All rights reserved.
doi:10.1016/j.jpowsour.2006.05.049

composition and the surface morphology of the SEI layer are examined by means of scanning electron microscopy (SEM) and X-ray photoelectron spectroscopy (XPS). The electrochemical performance of Si thin-film/Li half-cells with and without the FEC additive in ethylene carbonate/diethyl carbonate (EC/DEC, 3/7, v/v) containing 1.3 M $LiPF_6$ electrolyte is also investigated.

2. Experimental

A silicon thin-film electrode of 200 nm thickness was prepared by E-beam evaporation with a base pressure of $>1 \times 10^{-6}$ Torr.

The electrolyte solutions were commercially available 1.3 M lithium hexafluoro phosphate ($LiPF_6$) dissolved in ethylene carbonate (EC) and diethyl carbonate (DEC). The FEC additive was added at 3 wt.% to the EC/DEC (3/7, v/v) with 1.3 M $LiPF_6$.

The change in morphology of the silicon thin-film electrode with cycling in different electrolyte compositions was investigated by means of SEM (JEOL JSM-6700F). The surface structure of silicon electrode and the composition of the SEI layer derived from additive-containing electrolytes were analyzed by XPS (ESCA LAB 250).

The electrochemical properties of the silicon thin-film electrode were examined using a pouch half-cell (electrode area: 1 cm × 1 cm). The half-cells were fabricated by sandwiching a polyethylene separator (30 μm) between the silicon thin-film electrode and metallic lithium (100 μm, Cyprus Foote Mineral Co.). The separator accommodated the electrolyte solution. Cycle tests were performed with a galvanostatic charge–discharge tester (TOSCAT-3000, Toyo System Co.) in the voltage range 0.005–2.0 V at a constant current density of 0.04 mA cm^{-2} (*C*/5 rate). The 200-nm silicon thin-film electrode gave a capacity of 0.22 mAh cm^{-2} (based on the theoretical capacity of 4000 mAh g^{-1} for $Li_{4.2}Si$).

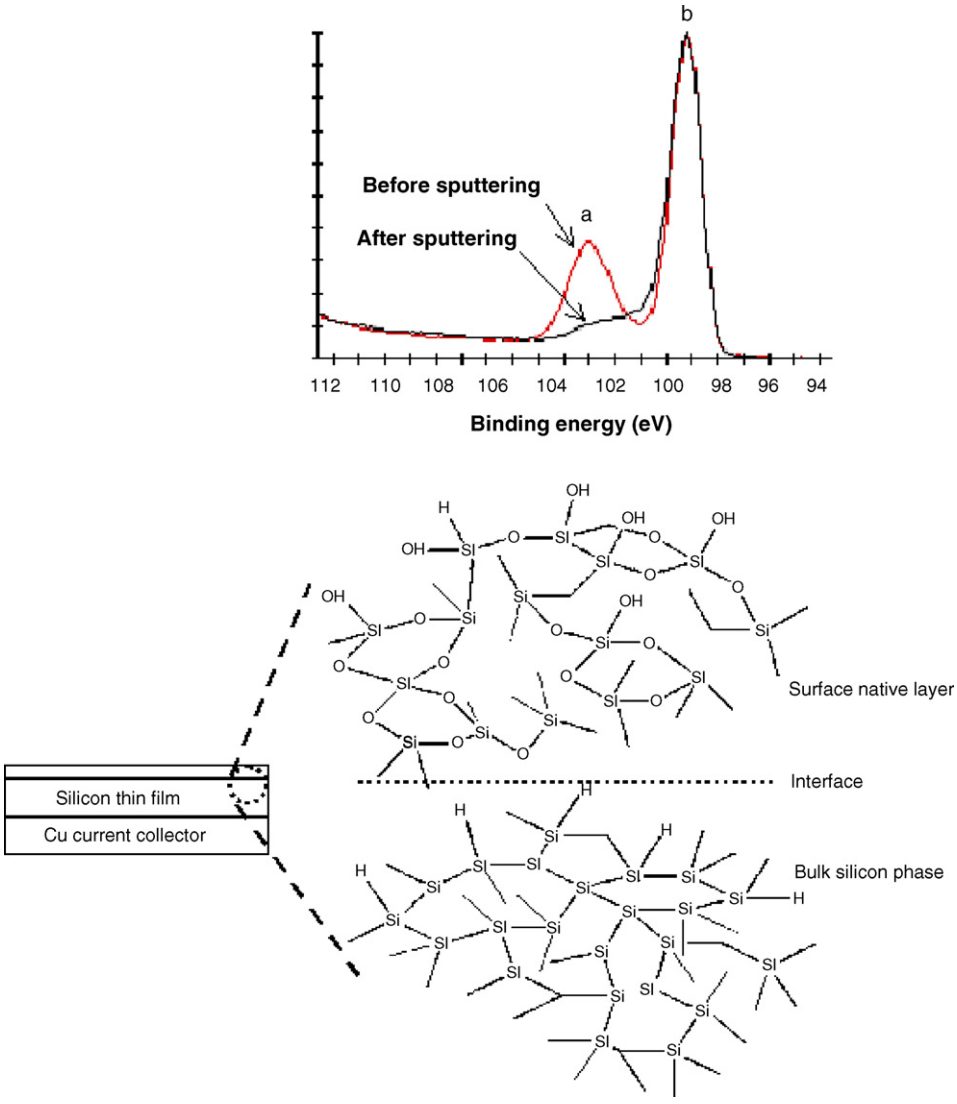

Fig. 1. XPS spectra for surface of silicon thin-film electrode before and after sputtering (Top) ((a) Si—O peak and (b) Si—Si peak). Schematic model of electrode with surface native layer and bulk silicon (Bottom).

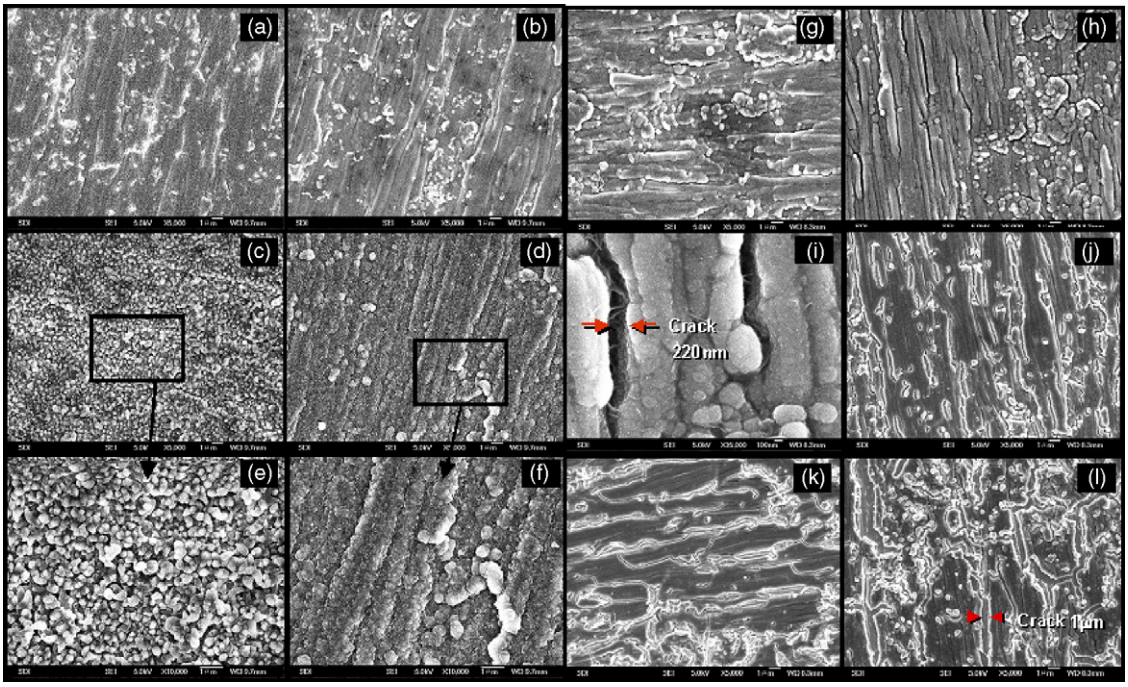

Fig. 2. Scanning electron micrographs of silicon thin-film electrode at different SoC and DoD: (a) initial state; (b) 100 min (0.281 V); (c) 400 min (0.0663 V); (d) 600 min charge (0.005 V); (e) ×10,000 of (c); (f) ×10,000 of (d); (g) 20 min; (h) 100 min; (i) ×35,000 of (h); (j) 400 min; (k) 500 min; (l) 600 min discharge.

3. Results and discussion

3.1. Native oxide layer of silicon thin-film electrode

The XPS spectra of the silicon thin-film electrode before and after argon sputtering are given in Fig. 1. The *a* peak of 103 eV and *b* peak of 99 eV correspond to –Si–O–Si– and –Si–Si–, respectively. From the disappearance of the –Si–O–Si– peak by sputtering, it is found that the surface of silicon thin-film electrode is covered with a 'native layer' consisting of the silicon oxide (–Si–O–Si–) and the silanol group (–Si–OH), as shown in the schematic model of Fig. 1. These compounds are produced by the reaction of silicon with O_2 or H_2O.

The native layer is thought to be responsible for the irreversible capacity, since during the first charge (lithium insertion) the silicon oxide layer with the silanol functional groups can react with the organic solvent, lithium salt, organic additive or impurities [14].

3.2. Change in surface morphology during cycling

Scanning electron micrographs showing the change in the morphology of the silicon thin-film electrode at different states of charge (SoC) and depths of discharge (DoD) are presented in Fig. 2. As shown in Fig. 2(e and f), a lithium alloy with a 200–500 nm sized particle-like shape is generated during the addition of lithium to the silicon thin-film electrode and the grains are aggregated due to the volume expansion at the full-charged state ($Li_{4.2}Si$ alloy). When the lithium is removed from the lithium alloy electrode, the electrode shrinks and produces the crack as shown in Fig. 2(h–l). The crack size is 220 nm after 100 min discharge (39.5% DoD) and about 1 μm after all available lithium is removed from the lithium alloy electrode, see Fig. 2(i and l).

In order to investigate the crack pattern under the prolonged cycling, SEM images were taken after 1, 10 and 80 cycles, as shown in Fig. 3. The cracking of the silicon thin-film electrode proceeds and the cracked silicon particle becomes smaller with cycle number. This can be attributed to the volumetric stresses of the active silicon phase that forms the alloy with lithium on the repeated cycling.

The cracking of active silicon phase continues during the repeated expansion and contraction of the electrode by the insertion and extraction of lithium or the breaking of the –Si–Si– network by irreversible reaction. In addition, the SEI layer is formed on the surface of the cracked silicon electrode by the reductive decomposition of the electrolyte solution and the morphology of the SEI layer may change due to the cracking of silicon electrode. These phenomena appear to lead to a moss-like, porous structure of the silicon electrode, as demonstrated in Fig. 3(d).

3.3. Surface modification by FEC additive

In order to investigate the effect of the FEC additive on the morphology of the silicon thin-film electrode after 80 cycles, a SEM image was obtained, see Fig. 3(e). The presence of FEC in the EC/DEC (3/7, v/v) with 1.3 M $LiPF_6$ electrolyte causes a less porous structure of the silicon electrode. The porous structure leads to marked complexity of the silicon electrode surface, with increased growth in the areas exposed to the electrolyte solution. Increasing surface area may cause an increase in the side reaction with the electrolyte. The formation of a non-uniform SEI layer in the cracked silicon phase can produce

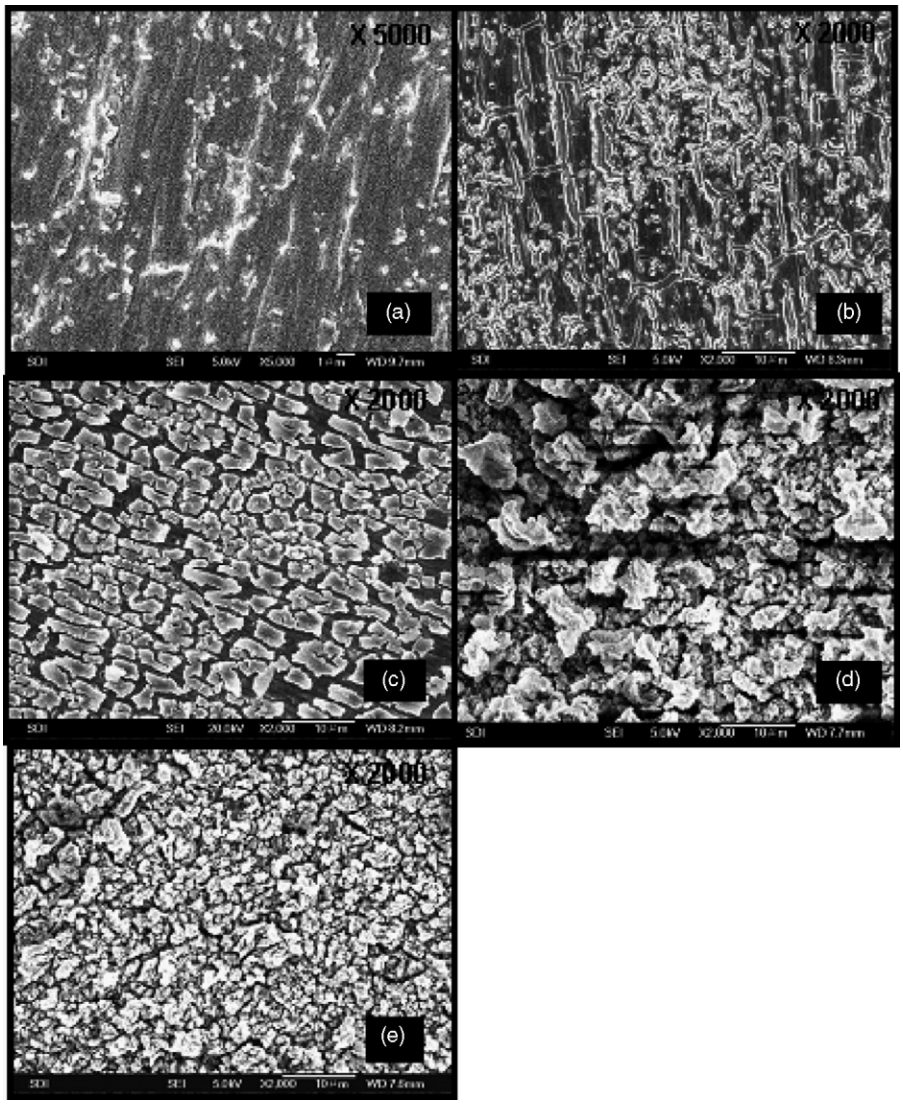

Fig. 3. Scanning electron micrographs of surface morphology of silicon thin-film electrode: (a) before cycling; after (b) 1 cycle; (c) 10 cycles; (d) 80 cycles (without FEC); (e) 80 cycles (with FEC).

the isolation of an active silicon phase, which leads to capacity loss.

To understand the morphology change of the silicon electrode with and without FEC, the surface components of the silicon electrode after cycling were investigated by XPS.

The XPS spectra of Si 2s and F 1s of the silicon electrode reacting with the electrolytes with and without FEC after 10 cycles are presented in Fig. 4. The Si 2s spectra contain a peak at 107 eV (corresponding to Si–F) for the electrolyte system with FEC. This peak is not observed in the absence of FEC, as shown in Fig. 4(a and b).

The F 1s spectra contain a peak at 686.5 eV (corresponding to LiF) for electrolyte both with and without FEC. The F 1s spectrum of the electrolyte without FEC has a much stronger shoulder at 688.5 eV (corresponding to $LiPF_6$ and LiP_xF_y) than that with FEC. This indicates that in the case of electrolyte without FEC less stable salts, like LiP_xF_y, are formed in the surface layer [6]. For the electrolyte with FEC, it is found that stable LiF is contained in the surface layer.

The surface layer at the interface between Si and the electrolyte without FEC contains EC-derivatives such as metastable linear alkyl carbonates (–Si–$OCH_2CH_2OCO_2Li$, –Si–$CH_2CH_2OCO_2Li$ $R(OCO_2Li)_2$). These compounds (–Si–C– (318 kJ mol^{-1}), –Si–O– (452 kJ mol^{-1})) are less dense and with cycling, can continue the decomposition due to the low bonding energy. The electrolyte can penetrate into the active silicon phase through the less dense surface layer during lithium insertion and break the –Si–Si– network bond (222 kJ mol^{-1}) by the reaction of lithium salt and organic solvent with silicon. This leads to cracking of the silicon electrode and the porous structure is generated, as shown in Fig. 3(d). From this result, it is clear that when an electrolyte with FEC is used, the SEI layer consists mainly of stable LiF and –Si–F (565 kJ mol^{-1}) compounds. These compounds do not decompose due to the high bonding energy and can maintain the stable interface on the prolonged cycling.

The reductive decomposition voltage of electrolyte with and without FEC was obtained from the dQ/dV (calculated differ-

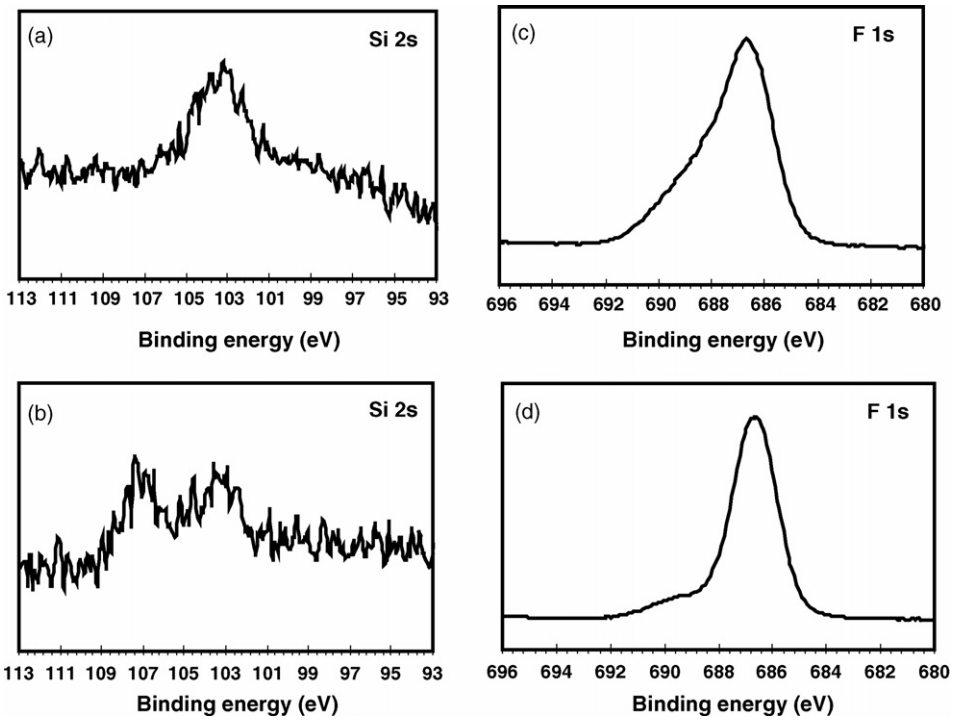

Fig. 4. XPS spectra for surface of silicon thin-film electrode: (a and c) EC/DEC (3/7, v/v) 1.3 M $LiPF_6$; (b and d) EC/DEC (3/7, v/v) 1.3 M $LiPF_6$ with 3 wt.% FEC.

ential capacity) plots of Fig. 5. The reductive decomposition of FEC (LUMO energy: 0.98 eV) is easier than that of EC (1.17 eV). The reduction of FEC progresses before that of EC and thereby an effective SEI layer can be produced at the Si|electrolyte interface.

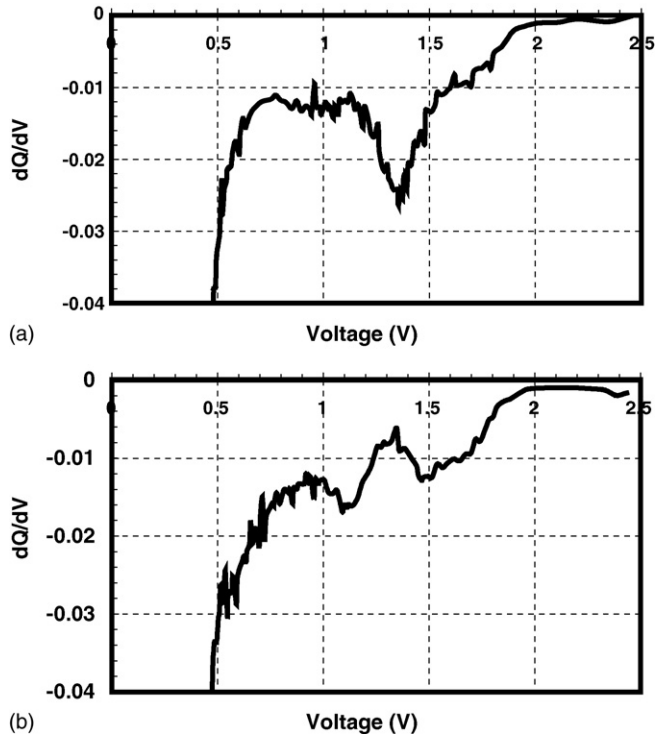

Fig. 5. dQ/dV plots of Si|Li half-cell with electrolyte of EC/DEC (3/7, v/v) 1.3 M $LiPF_6$: (a) without FEC; (b) with FEC.

3.4. Effect of FEC additive on electrochemical performance of Si|Li half-cell

Electrochemical cycling tests were conducted of Si|electrolyte|Li half-cells assembled with different electrolyte solutions. The results are summarized in Table 1. The ICE (initial coulombic efficiency) of the half-cell using the EC/DEC (3/7, v/v) 1.3 M $LiPF_6$ with 3 wt.% FEC as an electrolyte has a higher value of 88.7%. This implies a lower irreversible capacity, which is caused by trapping of lithium in the silicon electrode and lithium consumption through formation of the SEI layer.

The discharge capacity and coulombic efficiency of the Si|electrolyte|Li half-cell containing EC/DEC (3/7, v/v) 1.3 M $LiPF_6$ without FEC dramatically decay after 40 cycles, as shown in Fig. 6. In this case, the irreversible reaction consuming active lithium occurs continuously due to the unstable SEI layer, as shown in Fig. 4, and thus the capacity fades with cycle number. Retention of the discharge capacity of the Si|electrolyte|Li half-cell can be enhanced by the introduction of FEC additive to the electrolyte solution and the coulombic efficiency is also improved, as shown in Fig. 6(a and b).

Table 1
Initial coulombic efficiency and capacity retention at 80 cycles of a Si|electrolyte|Li half-cell with different electrolyte solutions

	EC/DEC (3/7) 1.3 M $LiPF_6$	EC/DEC (3/7) 1.3 M $LiPF_6$ with 3 wt.% FEC
Initial coulombic efficiency (%)	87.8	88.7
Discharge capacity retention (%)	67.9	88.5

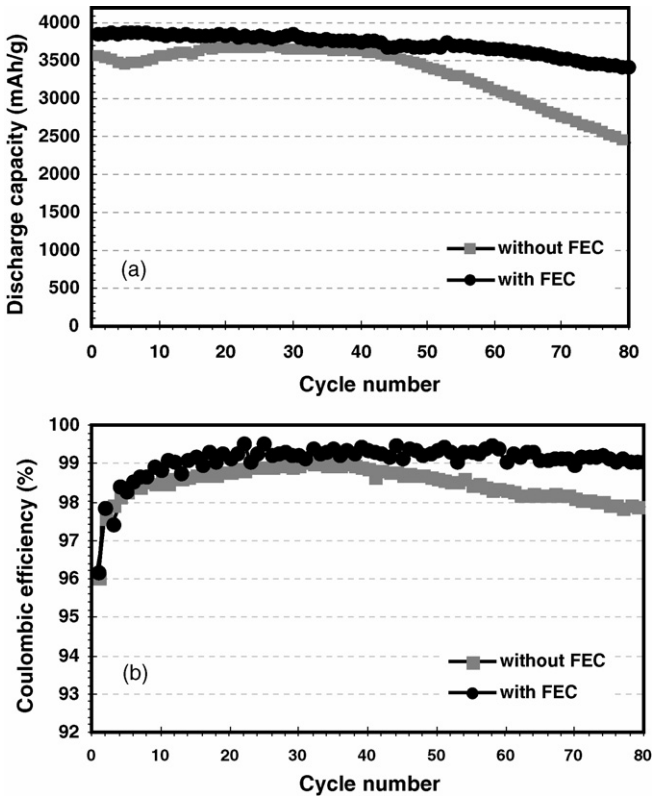

Fig. 6. Discharge capacity retention and coulombic efficiency of Si thin-film electrode|electrolyte|Li half-cell with cycle number. Charge cut-off: 0.005 V CC mode, discharge cut-off: 2.0 V CC mode, charge–discharge current rate: *C*/5.

4. Conclusions

It is found that a silicon thin-film electrode is covered with a less porous SEI layer by the introduction of 3 wt.% FEC additive to a EC/DEC electrolyte with 1.3 M $LiPF_6$. In FEC-free electrolyte, the SEI layer is relatively porous and rough. The presence of FEC can lead to a SEI layer which consists of stable compounds such as LiF and −Si−F and obviously improves the discharge capacity retention of the Si|Li half-cell (88.5% based on discharge capacity after 80 cycles). The coulombic efficiency of a half-cell with FEC-free electrolyte gradually decreases after 40 cycles, while that of a half-cell with electrolyte containing FEC is over 99% up to 80 cycles.

References

[1] J.P. Maranchi, A.F. Hepp, P.N. Kumta, Electrochem. Solid State Lett. 6 (9) (2003) A198–A201.
[2] H. Li, X. Huang, L. Chen, Z. Wu, Y. Liang, Electrochem. Solid State Lett. 2 (11) (1999) 547–549.
[3] T.D. Hatchard, J.R. Dahn, J. Electrochem. Soc. 151 (6) (2004) A838–A842.
[4] Z. Chen, V. Chevrier, L. Christensen, J.R. Dahn, Electrochem. Solid State Lett. 7 (10) (2004) A310–A314.
[5] M. Winter, J.O. Besenhard, Electrochim. Acta 45 (1999) 31–50.
[6] A.M. Andersson, M. Herstedt, A.G. Bishop, K. Edstrom, Electrochim. Acta 47 (2002) 1885–1898.
[7] B.V. Ratnakumar, M.C. Smart, S. Surampudi, J. Power Sources 97–98 (2001) 137–139.
[8] G.H. Wrodnigg, J.O. Besenhard, M. Winter, J. Electrochem. Soc. 146 (2) (1999) 470–472.
[9] H. Ota, Y. Sakata, A. Inoue, S. Yamaguchi, J. Electrochem. Soc. 151 (10) (2004) A1659–A1669.
[10] H. Yoshitake, K. Abe, T. Kitakura, J.B. Gong, Y.S. Lee, H. Nakamura, M. Yoshio, Chem. Lett. 32 (2) (2003) 134–135.
[11] R. Mogi, M. Inaba, S.-K. Jeong, Y. Iriyama, T. Abe, Z. Ogumi, J. Electrochem. Soc. 149 (12) (2002) A1578–A1583.
[12] R. McMillan, H. Slegr, Z.X. Shu, W. Wang, J. Power Sources 81–82 (1999) 20–26.
[13] K.-C. Moller, H.J. Santner, W. Kern, S. Yamaguchi, J.O. Besenhard, M. Winter, J. Power Sources 119–121 (2003) 561–566.
[14] J. Graetz, C.C. Ahn, R. Yazami, B. Fultz, Electrochem. Solid State Lett. 6 (9) (2003) A194–A197.